Wet/dry status change in global closed basins between the mid-Holocene and the Last Glacial Maximum and its implication for future projection

Xinzhong Zhang[1], Yu Li[1], Wangting Ye[1], Simin Peng[1], Yuxin Zhang[1], Hebin Liu[1], Yichan Li[1], Qin Han[1], Lingmei Xu[1]

[1]Key Laboratory of Western China's Environmental Systems (Ministry of Education), College of Earth and Environmental Sciences, Center for Hydrologic Cycle and Water Resources in Arid Region, Lanzhou University, Lanzhou 730000, China

Correspondence to: Yu Li (liyu@lzu.edu.cn)

Abstract. Closed basins, mainly located in subtropic and temperate drylands, have experienced alarming declines in water storage in recent years. An assessment of long-term hydroclimate change in those regions remains unquantified at a global scale yet. By integrating the lake records, PMIP3/CMIP5 simulations and modern observations, we assess the wet/dry status of global closed basins during the Last Glacial Maximum, mid-Holocene, pre-industrial, 20th and 21st century periods. Results show comparable patterns of general wetter climate during the mid-Holocene and near-future warm period, mainly attributed to the boreal summer and winter precipitation increasing, respectively. The long-term pattern of moisture change is highly related to the high-latitude ice sheets and low-latitude solar radiation, which leads to the poleward moving of westerlies and strengthening of monsoons during the interglacial period. However, modern moisture changes show correlations with ENSO in most closed basins, such as the opposite significant AI-MEI relationships between North America and Southern Africa and between Central Eurasia and Australia, indicating strong connection with ocean oscillation. The strategy for combating future climate change should be more resilient to diversified hydroclimate responses in different closed basins.

1 Introduction

A great number of observations in the last 100 years show that the Earth's climate is now experiencing significant change characterized by global warming (Hansen et al., 2010; Trenberth et al., 2013; Dai et al., 2015; Huang et al., 2016; Li et al., 2018), which is unequivocally induced by the increase in concentrations of greenhouse gases according to the Fifth Assessment Report of the Intergovernmental Panel on Climate Change (IPCC, 2013). Recent studies have indicated increasing drought and accelerated dryland expansion under modern global warming resulting from a higher vapour pressure deficit and evaporative demand (Dai, 2013; Feng and Fu, 2013; Huang et al., 2017). Assessing the impacts of global warming especially on the terrestrial moisture balance is not only one of the most important social and environmental issues but also the basis of future climate projections.

According to Held’s hypothesis, rising atmospheric humidity will cause the existing patterns of atmospheric moisture divergence and convergence to intensify, thereby making effective precipitation more negative in the drylands and more positive in the tropics, now referred to as the “dry gets drier, wet gets wetter” (DGDWGW) paradigm (Held & Soden, 2006; Hu et al., 2019). However, this mechanism may be more complex regionally, especially over terrestrial environments, where wet/dry pattern changes over the past decades and in future projections do not follow the proposed intensification trend (Greve et al. 2014; Roderick et al. 2014). To accurately project future terrestrial hydroclimatic changes, past climates may aid in understanding the regional nuances of the DGDWGW effect (Lowry & Morrill, 2019). Quade and Broecker (2009) have verified Held’s hypothesis by taking the Last Glacial Maximum (LGM) as a reverse analog for modern global warming, and point out that the hydroclimate changes in subtropical regions are more complicated. Besides, the African Humid Period and a following mid-Holocene (MH) thermal maximum are also the focused key periods (Lézine et al., 2011), and related researches prove that gradual climate forcing can result in rapid climate responses and a remarkable transformation of the hydrologic cycle (deMenocal & Tierney, 2012). Furthermore, Burke et al. (2018) compared the six warm periods in the past including the early Eocene, mid-Pliocene, Last Interglacial, mid-Holocene, pre-Industrial (PI) and 20th century with the simulated future scenario to find the best analog for near-future climate. A long-term and large-scale evaluation on global hydroclimate change is of vital significance for a comprehensive understanding of the impact of global warming and for future climate projections.

Closed basins account for about one fifth of the global land areas and are mainly located in the arid and semi-arid climate zones. As there is no outlet or hydrological connection to the oceans, the terminal lakes function as the ocean for closed basins and concentrate the sedimentary information of the whole basin (Li et al., 2015), which makes them ideal candidates for studying the hydroclimate change of the past. Besides, they play an important role in mitigating global changes by influencing the trend and interannual variability of the terrestrial carbon sink (Ahlström et al., 2015; Li et al., 2017), though the hydrological cycle of the closed basins is fragile and sensitive to climate change. In the most recent IPCC sea level budgets, changes in terrestrial water storage driven by the climate have been assumed to be too small to be included (IPCC, 2013; Zhan et al., 2019). However, recent advances in gravity satellite measurement enabled a quantification that water storages in closed basin are declining at alarming rates, which not only exacerbate local water stress, but also impose excess water on exorheic basins, leading to a potential sea level rise that matches the contribution of nearly half of the land glacier retreat (excluding Greenland and Antarctica) (Wurtsbaugh et al., 2017; Wang et al., 2018). The influence of global warming on water availability in closed basins is far more serious than that in other regions, and understanding the pattern and mechanism of hydroclimate change in the past and modern warm periods will be the key to assess the impact of future climate change.

In this paper, we focus on the wet/dry status change between the LGM, MH and modern warm period in global closed basins to improve our knowledge of regional responses to climate change. Based on the lake records, modern observations and simulations of the key periods from the Paleoclimate Modeling Intercomparison Project Phase 3 (PMIP3) and Coupled Model Intercomparison Project Phase 5 (CMIP5), an assessment of hydroclimate change at different timescales from the LGM to MH and from the PI to late 21st century is conducted. The possible linkages of these moisture change patterns and their underlying physical mechanisms are also discussed. This assessment is essential for future climate projection and regional water management, especially in the dry hinterland.

2 Data and methods

2.1 Water level and moisture change inferred from lake records

The following criteria were used for the selection of the proxy records in this study (Chen et al., 2015): (1) The proxies should be indicative of moisture changes. (2) The records should cover both the LGM and MH time slices. (3) The dominant driving mechanism of the variation in proxy records should be climatic changes. (4) The records should have a dating control level of 6 or better for 21 ka and 6 ka time slices according to the Cooperative Holocene Mapping (COHMAP) project dating scheme. A dating control level of 6 for continuous sequences was based on the following criteria: Bracketting dates, one within 6000 years and the other within 8000 years or one within 4000 years and the other within 10000 years of the selected date (21 ka and 6 ka). The same control level applied to discontinuous sequences requires at least one date within 2000 years of the time being assessed (Street-Perrott et al., 1989; COHMAP Members, 1994; Lowry & Morrill, 2019).

We then compared our new compilation of proxy records (Supplement Table S1) to 50 water level records from the Global Lake Status Data Base (Street-Perrott et al., 1989; COHMAP Members, 1994; Kohfeld and Harrison, 2000; Harrison et al., 2003) and Chinese lake-status database (Yu et al., 2001; Xue et al., 2017) in global closed basins and surrounding areas (Fig. 1). To capture the general spatial pattern, the differences of lake status between the LGM and MH in individual records were classified into 3 grades (higher/wetter, moderate, lower/drier). Similarly, the differences of simulated effective precipitation between the LGM and MH from PMIP3/CMIP5 multi-models in certain grid of the lake site were classified into positive, no change and negative and compared with the records.

2.2 Modern data sources and analyses

Closed basin extents were acquired from HydroBASINS product, a series of polygon layers that depict watershed boundaries and sub-basin delineations at a global scale by using the HydroSHEDS (Hydrological data and maps based on SHuttle Elevation Derivatives at multiple Scales) database at 15 arc-second resolution (Lehner et al., 2013). There were some exceptions we did not take them into account in this study: (1) Ten landlocked watersheds in the Inner Tibetan Plateau, Northeast China, Siberia and western United States were captured only in Global Drainage Basin Database (Masutomi et al., 2009; Wang et al., 2018); (2) Sporadic landlocked watersheds smaller than 100 km^2 Embedded in the exorheic regions were not considered as independent units; (3) Some of the contemporary endorheic watersheds were exorheic in the past, such as the Wuyuer river basin in Northeast China.

Primary variables of mean precipitation (P) and potential evapotranspiration (PET) from Climatic Research Unit Time-Series version 4.01(CRU TS4.01), a gridded time-series dataset of month-by-month variation in climate covering all land areas (excluding Antarctica) at 0.5° resolution over the period 1901-2016 (Harris et al., 2014), were used for modern climate analysis.

Aridity index (AI) defined as the ratio of annual precipitation to annual potential evapotranspiration by the United Nations Environment Programme (UNEP, 1992) was applied. Furthermore, to explore the possible relationship between the ocean and closed basins in modern times, we carried out the pearson correlation analysis between monthly AI and multivariate El Niño/Southern Oscillation (ENSO) index (MEI) (Kobayashi et al., 2015) and other indexes such as the North Atlantic Oscillation (NAO), Southern Oscillation Index (SOI), Pacific Decadal Oscillation (PDO) and Tripole Index for the Interdecadal Pacific Oscillation (TPI) (Supplement Table S2) for different endorheic regions. Linear trend of AI change in global closed basins during 1979-2016 was provided, and a trend was considered statistically significant at a significance level of 5%.

2.3 Debiasing and downscaling of PMIP3/CMIP5 multi-model ensemble

Experiments of the LGM, MH and PI from the PMIP3 and projection experiment of 21st century under Representative Concentration Pathway 8.5 (RCP8.5) from the CMIP5 were used in this study (Braconnot et al., 2012; Taylor et al., 2012). To ensure the consistency and precision of simulations as much as possible, we used the outputs from 5 global climate models (Table 1) which have all completed the above key period experiments at a spatial resolution of less than 3 degrees. The periods of 2006-2015 and 2091-2100 were defined as the representatives of early and late 21 century (E21 and L21), respectively.

Statistical downscaling and debiasing followed a multi-step approach described by Tabor and Williams (2010). The primary climate variables were first debiased by differencing each paleoclimate (LGM, MH, PI) or future climate (2017-2100) simulation from a present climate simulation (2006-2015). These anomalies are then downscaled through spline interpolation to a 0.5° resolution grid corresponding to the modern observational CRU dataset. The anomalies are then added to the observational data (2006-2015) to produce the debiased and downscaled primary variables for the paleoclimate or future climate simulation. This differencing removes any systematic difference as long as that bias is constant through time (Wilby et al,. 2004; Lorenz et al., 2016). The effective precipitation calculated by precipitation minus evaporation was introduced to compare with the lake status during the LGM and MH, and predict future changes in moisture balance.

Table 1. PMIP3/CMIP5 models used in this study.

Model name	Resolutions	Modelling centre	References
CCSM4	288×192	National Center for Atmospheric Research, USA	(Gent et al., 2011)
CNRM-CM5	256×128	Centre National de Recherches Meteorologiques, France	(Voldoire et al., 2013)
GISS-E2-R	144×90	NASA Goddard Institute for Space Studies, USA	(Schmidt et al., 2014)
MIROC-ESM	128×64	Japan Agency for Marine-Earth Science and Technology, Japan	(Watanabe et al., 2011)
MRI-CGCM3	320×160	Meteorological Research Institute, Japan	(Yukimoto et al., 2012)

3 Results

3.1 Wet/dry status changes from lake records

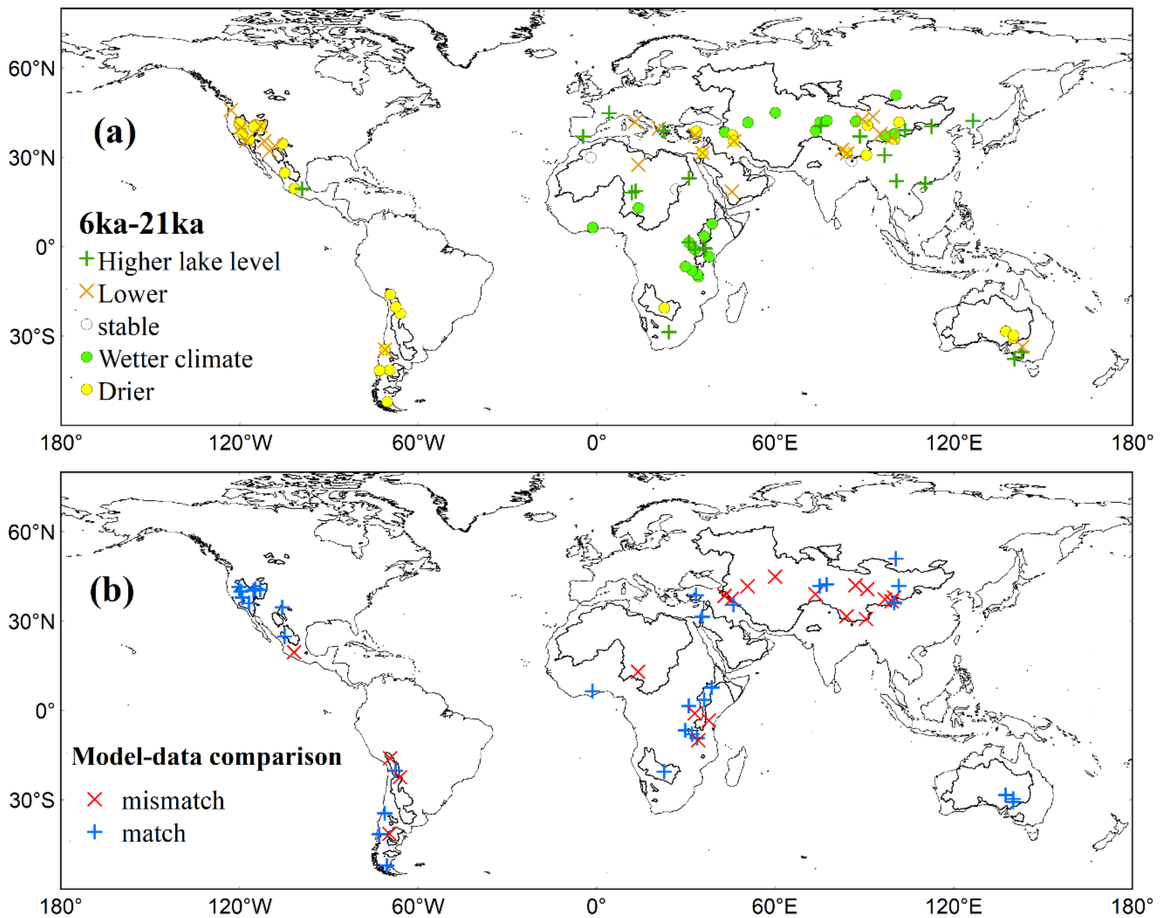

Figure 1. Wet/dry status changes between the LGM and MH from lake records (a) and comparison with the simulated effective precipitation from PMIP3/CMIP5 multi-models (b). The green and yellow cross sites are from lake status databases; the green and yellow point sites are from recently published literatures; the hollow points indicate that there is no significant change in lake level or climate condition between the LGM and MH.

Generally, lake level changes match climate changes from the proxy records well (Fig. 1a), except for Western China where many hydroclimate records from different lakes remain controversial. In the North and South American continents, almost all closed basins experience a wetter LGM compared to the MH status, and the same situations exist in some closed basins of Eastern Mediterranean, Tibetan Plateau and Australia. On the contrary, Eastern African highlands and the Sahel region show a prevailing wetter MH, which may be highly attributed to the African Humid Period. Changes in Central Eurasia are more complicated. The monsoonal Eastern Asia and arid Central Asia both record wetter MH, while in the middle area between them, there are some contradictory records synchronously showing lower lake level and wetter climate. Though evidence from Southern Africa and Australia are insufficiency, several records tend to support a wetter LGM. Hereto, it is worth noting that there are two belt regions around latitude 30 degrees at both Hemisphere where substantial high lake levels during the LGM have disappeared or subsided during the MH. And the low-latitude Africa and mid-latitude Asia basically experience an opposite pattern of a wetter MH.

Comparison between the wet/dry status change from new compilation of proxy records and simulated effective precipitation from PMIP3/CMIP5 multi-models is shown in Fig. 1b. The model ensemble does particularly well in simulating the direction of hydroclimate change in most closed basins of Americas, Africa and Australia. The most mismatches exist in the Central Eurasia, since many lake records suggest wetter climate during MH whereas the model ensemble does not. Some minor mismatches occur in the East Africa and South America, where the altitude changes dramatically so that the models may appear to miss the details of climate change.

3.2 Simulated climate changes under the past and future warming

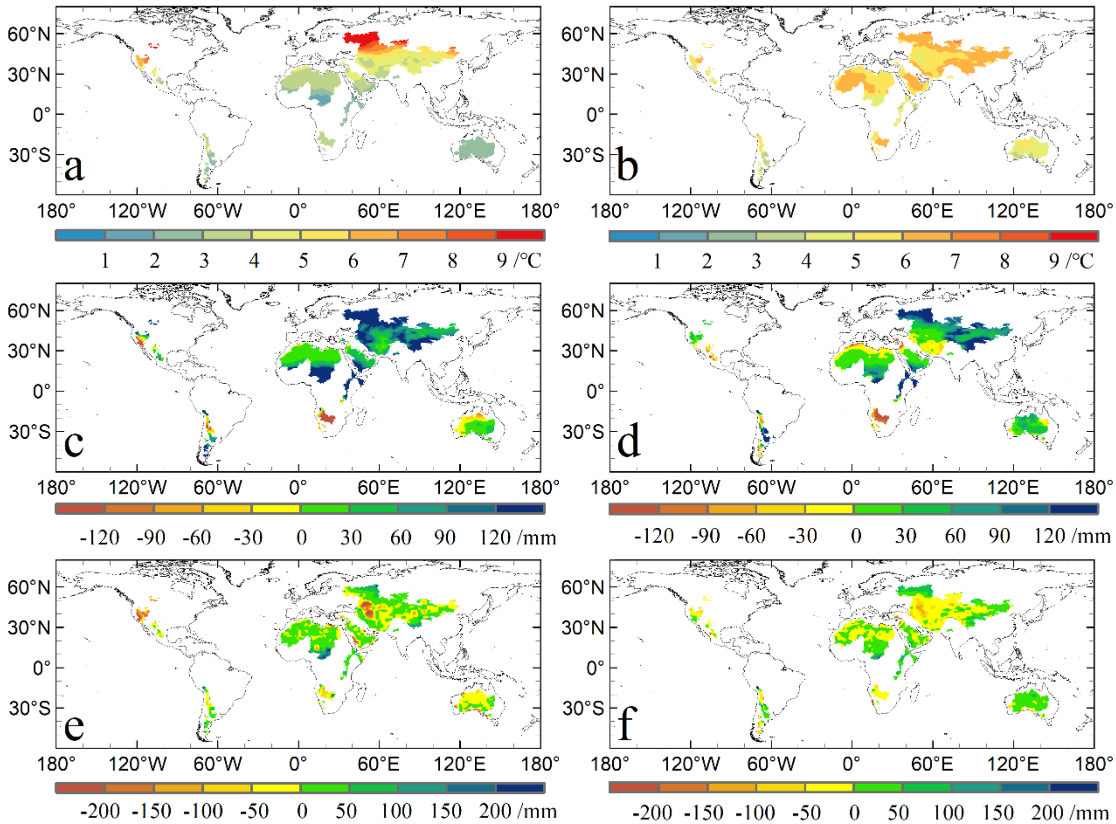

Figure 2. Annual mean temperature (a,b), precipitation (c,d) and effective precipitation (e,f) differences for MH-LGM (left) and L21-PI (right) in global closed basins based on the PMIP3/CMIP5 multi-model ensemble.

Spatial patterns of hydroclimate change for MH-LGM and L21-PI are shown in Fig. 2. It's apparent that the MH warming is characterized by strong latitudinal zonality, while future warming is more homogeneous over all closed basins.The temperature rise by the end of this century will exceed that during the period of LGM-MH in most closed basins under RCP8.5 scenario (excluding the high latitudes of North America and Central Asia). On the contrary, precipitation increasing under future warming is lighter and keep the similar distribution pattern of MH. The dramatic shifts of precipitation change bettwen the two periods exist in the subtropics such as the dry-wet shifts in the Mediterranean coast, Mexican Plateau and Iranian Plateau. For the pattern of effective precipitation change, it's substantially fragmented. The prevailing wetter climate in North Africa and Central Eurasia during the MH is weakened while Australia gets wetter in the future. As a consequence, the core area of drought is moved from Western America during the MH to Central Asia by the end of this century.

Table 2. Percentage changes of monthly precipitation and evaporation between different periods from the multi-models.

		1	2	3	4	5	6	7	8	9	10	11	12
MH-LGM	P	8.3	2.0	-1.1	9.7	25.8	32.1	41.1	52.7	57.5	46.0	34.8	18.1
	E	17.1	11.0	10.9	16.0	27.4	36.1	40.2	43.7	42.4	35.9	30.7	24.9
L21-PI	P	10.8	12.1	12.6	14.4	8.3	-1.5	1.5	6.5	8.3	11.3	11.6	11.4
	E	9.5	10.2	11.6	14.5	12.8	9.5	6.5	7.9	6.8	4.9	6.5	9.5
L21-E21	P	9.3	7.7	8.9	12.7	7.3	-1.0	4.6	8.2	6.2	8.0	6.5	7.9
	E	8.4	7.9	8.3	12.0	10.7	8.8	6.7	8.4	6.7	5.4	4.6	7.1

To investigate the seasonal difference of hydroclimate change, we assess the percentage changes of monthly precipitation and evaporation during the MH, modern and future warm periods at a global scale (Table 2). It turns out that remarkable increases of precipitation and evaporation mainly occur in the boreal summer half-year during the MH, while in modern and future warm periods they are concentrated in the boreal winter half-year. The precipitation increases more than 50% from the LGM to the MH in the wettest months of July-September, 13% from PI to L21 in the wettest months of February to April. Seasonal variation in evaporation is far smaller than that in precipitation, nonetheless, they both tend to diminish in the future.

3.3 Moisture trends and connections of modern observations

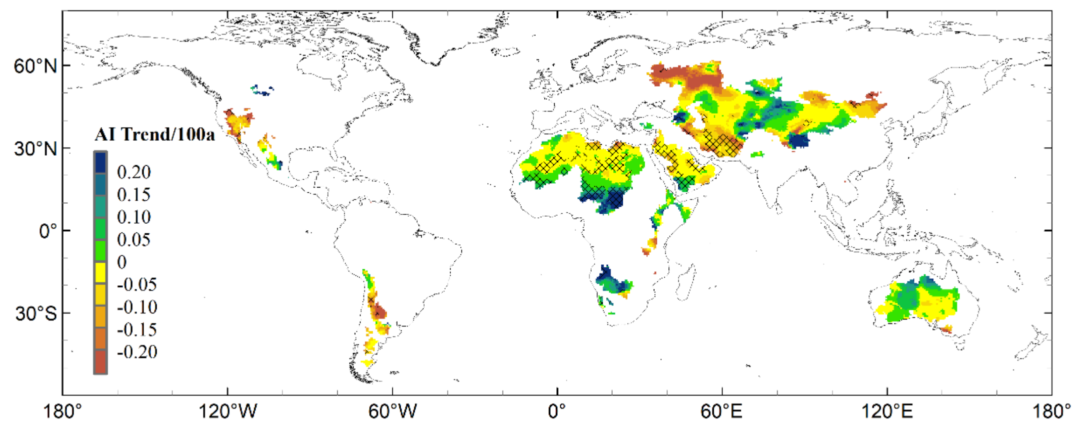

Figure 3. Linear trends of modern observational AI for the period of 1979-2016 in global closed basins. Gridding areas are where the trends are statistically significant at 5% level.

Over the past four decades, as shown in Fig. 3, about 70% of the total areas of global closed basins are getting drier. The severe drying regions include the Great Basin and the Patagonia in Americas and the Upper Volga river basin and Iran Plateau in Central Eurasia. The wetting trends mainly occur in the low latitudes of Africa and the high altitudes of Asia including the Caucasus Mountains, the Tianshan Mountains, the Pamir and Tibetan Plateau. Besides, the marginal closed basins of East Asia and North Australia as well as the Mexican Plateau and the Altiplano in the Americas show lighter wetting trends. It's worth noting that the future pattern of effective precipitation change (Fig. 2f) mainly continues the trends of modern moisture change, with the most significant mismatch in Southern Africa. That means the mechanism of future hydroclimate change likely keep the same as modern times in most closed basins.

Table 3. Pearson correlation coefficients between annual AI and monthly MEI during 1979-2016. The bold numbers mean that correlation coefficients are statistically significant at 5% level. SAM-South America, NAM-North America, SAF-Southern Africa, EAF-Eastern Africa, NAF-Northern Africa and Arabian peninsula, CEA-Central Eurasia, AUS-Australia, ALL-global closed basins.

	1	2	3	4	5	6	7	8	9	10	11	12
SAM	-0.23	-0.26	-0.15	-0.05	-0.05	0.08	0.22	0.29	0.27	0.22	0.14	0.19
NAM	**0.47**	**0.52**	**0.55**	**0.50**	**0.47**	0.30	0.06	-0.02	0.01	-0.01	-0.01	-0.02
SAF	**-0.60**	**-0.57**	**-0.60**	**-0.64**	**-0.53**	**-0.37**	-0.15	0.01	-0.07	-0.10	0.00	0.00
EAF	-0.02	-0.06	-0.12	-0.07	0.01	-0.01	-0.02	0.08	0.10	0.16	0.25	0.28
NAF	0.03	0.01	-0.03	-0.09	-0.09	-0.05	0.00	0.01	0.05	0.10	0.14	0.11

CEA	0.19	0.16	0.13	0.19	0.31	**0.45**	**0.50**	**0.47**	**0.47**	**0.45**	**0.43**	**0.41**
AUS	0.06	0.09	0.09	0.13	0.06	-0.13	-0.28	-0.28	**-0.32**	**-0.34**	**-0.37**	**-0.36**
ALL	-0.02	-0.05	-0.09	0.02	0.13	0.24	0.30	**0.38**	**0.36**	**0.37**	**0.41**	**0.42**

By calculating the pearson correlation coefficients between annual AI and monthly MEI, NAO, SOI, PDO and TPI, we seek for the potential connections of moisture change in closed basins with ocean oscillation. As results, the performance of NAO, SOI and PDO are comparatively weak, and the MEI responds the best and shows the similar pattern as TPI does, both indicating the dominant role of the Pacific Ocean oscillation in controlling the moisture change of global closed basins (Table 3, Supplement Table S2). For the global closed basins as a whole, the AI change is significantly positive related to monthly MEI from August to December, and the correlation coefficient reaches its highest in December of boreal winter season. As the biggest part of global closed basins, Central Eurasia apparently contributed the most in this positive feedback. On the contrary, in the Australian closed basins it's lightly negative correlated with monthly MEI during almost the same seasons. Among the seven separated endorheic regions, AI changes in South America, Eastern and Northern Africa show no significant correlation with MEI at all. For the other four regions, they are seemingly coupled between North America and Southern Africa and between Central Eurasia and Australia with the opposite significant AI-MEI relationships. During the first half year, North America responds positively whereas Southern Africa shows negative response to the MEI change. The same pattern turns to Central Eurasia and Australia in the second half year. This provides a potential perspective on the teleconnections in different closed basins globally.

4 Discussion

Closed basins are mainly located in subtropic and temperate drylands, which determines the limited moisture transport via atmospheric circulation. Based on that, Among the seven separated endorheic regions mentioned before, most of them can be divided into two parts: the westerlies-dominated area and the monsoon-influenced area, such as Central Asia and East Asia in Central Eurasia as well as the Western United States and the Mexican Plateau in North America. Thus, their climate changes are strongly influenced by the interactions of mid-latitude westerlies and low-latitude monsoon especially on a long-term timescale. Given the position of westerlies and strength of monsoons in modern times have no chance to change dramatically as in the last deglaciation, the oceans rather than the Earth orbital forcing start to play more important roles in controlling the regional moisture change. Even so, hydroclimate change in some closed basins respond in the same pattern to the past and future warming, indicating deeper connections between different timescales. More importantly, the long-term hydroclimate change patterns provide the baseline for modern and future climate change assessment.

From the perspective of paleoclimatology, the early and middle Holocene were characterised by the dramatic strengthening of monsoons and the retreat of ice sheets corresponding to the global warming. Evidences from the paleoclimate and archaeological records in Northern Africa had shown that the world's largest desert in modern times was covered by numerous forests and lakes paced by earth's orbital changes during the early Holocene (deMenocal & Tierney, 2012). Positive hydroclimate change in the Northern and Eastern Africa have already verified by the studies on the strengthening of the West African monsoon during the MH (Lézine et al., 2011; deMenocal & Tierney, 2012), and this kind of shifts were recorded in many monsoonal regions globally. As the most typical one, Asian monsoon even reached as far as the west Tianshan Mountains of Central Asia during the early and middle Holocene (Wang et al., 2014), bringing monsoon precipitation and affecting the hydroclimate pattern in the eastern closed basins of Central Eurasia. Another example are the Australian closed basins which were significantly affected by the subtropical Australian monsoon. Due to the precipitation increasing in the northern upstream basin, the water level of Lake Eyre in the early and middle Holocene reached the highest during the past 30 thousand years (Magee et al., 2004). Similarly, high lake levels and a wetter climate returned during the MH over North American monsoonal region, however, some studies suggested that this trend is caused by the destruction of vegetation by early human activities (Bridgwater et al., 1999; Caballero et al., 1999). In addition, it was also considered that the increase of atmospheric CO_2 concentration was the main driving force for the changes of climate and lake level since the LGM (Shakun et al., 2010; Li et al., 2013).

Moisture changes in Central Euraisa are more complicated due to the interactions of westerlies and monsoon in the middle region between the arid Central Asia and monsoonal Eastern Asia. During the LGM period, the westerlies in the Northern Hemisphere moved south reaching the southwest of the United States, the eastern Mediterranean region and southern Tibetan Plateau, because of the development of continental ice sheet in the North Hemisphere such as the Laurentian Ice Sheet (Claire et al., 2010; Lachniet et al., 2014; Lowry & Morrill, 2019). As a consequence, the effective precipitation in the arid Central Asia didn't increase until the middle and late Holocene, leading to a large number of low lake levels. After that, due to the increase of summer solar radiation in the Northern Hemisphere during the early and middle Holocene, a stronger East Asian monsoon brought more precipitation and high lake levels, showing different climate response patterns compared with that in the arid Central Asia (Chen et al., 2008; Ran et al., 2013; Huang et al., 2014). This difference in moisture change between the arid Central Asia and monsoonal Eastern Asia still exists in modern times and near-future warm period, and it is more apparent between the high altitudes and lower basins from the modern observations. Based on the simulation of future climate change, evidence shows that the winter precipitation play a dominant role in determining the wet/dry pattern change in global closed basins, implying the significance of westerly instead of monsoon.

Previous studies have indicated that the hydroclimate change patterns in different latitudes at the millennial, centurial and decadal timescales show considerable connection with the general atmospheric circulation, which is mainly forced by the external forcing at a long-term timescale and by the internal factors of climate system at a shorter timescale (Tierney et al., 2013; Ljungqvist et al., 2016; Zhang et al., 2017; Kohfeld et al., 2013). As results shown before, ocean oscillation especially the Pacific Ocean oscillation emphasize its impact on controlling the moisture change of global closed basins, with two couples of the opposite significant AI-MEI relationships between the North America and the Southern Africa and between the Central Eurasia and the Australia. It is well known that during an ENSO warm event, drought occurs in regions of northeastern Australia, leading to anomalously low annual rainfall (Cai et al., 2001; King et al., 2014). Thus the precipitation or runoff from the upstreams in the north mainly control the moisture fluctuations in the Australian closed basins. Also, the ENSO-based composite analyses have shown that the water vapor fluxes of seasonal precipitation in Central Eurasia are mainly generated in Indian and North Atlantic Oceans and transported by enhanced westerlies during EI Nino (Xi et al., 2018; Rana et al., 2017). These patterns provide some new perspectives to understand the differences and connections over global closed basins. And that reminds us that we should focus more on the ocean oscillations in order to address the challenges of future climate change.

5 Conclusion

This study presents a new compilation of lake records and analyses of hydroclimate change at different timescales in global closed basins. Though it's well known that the forcing mechanisms between mid-Holocene and future warming are different, the patterns of hydroclimate changes of them show comparable spatial consistency in closed basins. From the LGM to the MH, the westerlies-dominated areas usually experience wet to dry shift whereas the monsoon-influenced areas shift from drier to wetter climate. The hydroclimate changes from the PI to the Late 21st century show the similar patterns in most closed basins, except for Central Asia where it is wetter during the MH but drier during the future warm period. For the global closed basins as a whole, it's wetter both in the MH and L21 than that during the LGM and PI. However, they are mainly attributed to the boreal summer and winter precipitation increasing, respectively. The seasonal difference of precipitation increasing indicates the different dominant roles of westerly winds and monsoons during the two periods. That is, the long-term regional differences of hydroclimate change are mainly controlled by the high-latitude ice sheets and low-latitude solar radiation, which leads to equatorward moving of the westerlies during the glacial period and the strengthening of monsoons during the interglacial period. An analynis of modern moisture change matching with the timescale of future warming suggests that it's related to ocean oscillations especially the Pacific Ocean oscillation, such as the two coupled opposite significant AI-MEI relationships between the North America and the Southern Africa and between the Central Eurasia and the Australia. Though the dryland expansion may be accelerated under the near future warming in the hinterland globally, we can't ignore the hydroclimate response differences within these regions, which largely affect the local strategies of economic development and environmental protection. We must be more resilient to tackle the future climate change corresponding to diversified hydroclimate changes in different closed basins.

Data Availability. Boundaries of closed basins are available from the Hydrological data and maps based on SHuttle Elevation Derivatives at multiple Scales (HydroSHEDS) website https://www.hydrosheds.org/page/hydrobasins. The Global Lake Status Data Base and Chinese lake-status database are available from the Paleoclimatology Datasets of NOAA's National Centers for Environmental Information (NCEI) https://www.ncdc.noaa.gov/data-access/paleoclimatology-data/datasets. PMIP3/CMIP5 simulations are available from the Earth System Grid Federation (ESGF) Peer-to-Peer (P2P) enterprise system website https://esgf-node.llnl.gov/projects/esgf-llnl/. CRU TS4.01 data are available from https://crudata.uea.ac.uk/cru/data/hrg/. The

Values of MEI, NAO, SOI, PDO and TPI are available from https://psl.noaa.gov/data/climateindices/list/. Details about the new compilation of proxy records are available in Supplement.

Author contributions. Yu Li and Xinzhong Zhang designed this study and carried it out. Wangting Ye, Yuxin Zhang and Simin Peng contributed to the data processing, analysis and discussion of results. Xinzhong Zhang prepared the manuscript with contributions from all co-authors.

Competing interests. The authors declare that they have no conflict of interest.

Acknowledgements. This work was supported by the National Natural Science Foundation of China (Grant Nos. 41822708 and 41571178), the Strategic Priority Research Program of Chinese Academy of Sciences (Grant No. XDA20100102), the Fundamental Research Funds for the Central Universities (Grant No. lzujbky-2018-k15) , and the Second Tibetan Plateau Scientific Expedition (STEP) program (Grant No. XDA20060700).

References

Ahlström, A., Raupach, M. R., Schurgers, G., Smith, B., Arneth, A., Jung, M., Reichstein, M., Canadell, J. G., Friedlingstein, P., Jain, A. K., Kato, E., Poulter, B., Sitch, S., Stocker, B. D., Viovy, N., Wang, Y., Wiltshire, A., Zaehle, S., & Zeng, N. (2015). The dominant role of semi-arid ecosystems in the trend and variability of the land CO2 sink. Science, 348(6237), 895-899.

Braconnot, P., Harrison, S. P., Kageyama, M., Bartlein, P. J., Masson-Delmotte, V., Abe-Ouchi, A., & Zhao, Y. (2012). Evaluation of climate models using palaeoclimatic data. Nature Climate Change, 2(6), 417.

Bridgwater, N. D., Heaton T. H. E., & O'hara, S. (1999). A late Holocene palaeolimnological record from central Mexico, based on faunal and stable-isotope analysis of ostracod shells. Journal of Paleolimnology, 22(4), 383-397.

Burke, K. D., Williams, J. W., Chandler, M. A., Haywood, A. M., Lunt, D. J., & Otto-Bliesner, B. L. (2018). Pliocene and Eocene provide best analogs for near-future climates. Proceedings of the National Academy of Sciences, 115(52), 13288-13293.

Caballero, M., Lozano, S., Ortega, B., Urrutia, J., & Macias, J. L. (1999). Environmental characteristics of Lake Tecocomulco, northern basin of Mexico, for the last 50,000 years. Journal of Paleolimnology, 22(4), 399-411.

Cai, W., Whetton, P. H., & Pittock, A. B. (2001). Fluctuations of the relationship between enso and northeast australian rainfall. Climate Dynamics, 17(5-6), 421-432.

Chen, F., Yu, Z., Yang, M., Ito, E., Wang, S., Madsen, D. B., & Boomer, I. (2008). Holocene moisture evolution in arid central Asia and its out-of-phase relationship with Asian monsoon history. Quaternary Science Reviews, 27(3-4), 351-364.

Chen, J., Chen, F., Feng, S., Huang, W., Liu, J., & Zhou, A. (2015). Hydroclimatic changes in China and surroundings during the Medieval Climate Anomaly and Little Ice Age: spatial patterns and possible mechanisms. Quaternary Science Reviews, 107, 98-111.

Claire, M. C., & Rambeau. (2010). Palaeoenvironmental reconstruction in the southern levant: synthesis, challenges, recent developments and perspectives. Philosophical Transactions of the Royal Society A: Mathematical, Physical and Engineering Sciences, 368, 5225-5248.

COHMAP Members. (1994). Oxford Lake Levels Database. IGBP PAGES/World Data Center- A for Paleoclimatology Data Contribution Series # 94-028. NOAA/NGDC Paleoclimatology Program, Boulder CO, USA.

Cook, K. H. (2000). A southern hemisphere wave response to enso with implications for southern africa precipitation. Journal of Atmospheric Sciences, 58(15), 2146-2162.

Dai, A. (2013). Increasing drought under global warming in observations and models. Nature Climate Change, 3(1), 52-58.

Dai, A., Fyfe, J. C., Xie, S. P., & Dai, X. (2015). Decadal modulation of global surface temperature by internal climate variability. Nature Climate Change, 5(6), 555-559.

deMenocal, P. B., & Tierney, J. E. (2012). Green Sahara: African humid periods paced by earth's orbital changes. Nature Education Knowledge, 3(10), 12.

Feng, S., & Fu, Q. (2013). Expansion of global drylands under a warming climate. Atmospheric Chemistry and Physics, 13(10), 081-100.

Garcia, D. (2010). Robust smoothing of gridded data in one and higher dimensions with missing values. Computational statistics & data analysis, 54(4), 1167-1178.

Gent, P. R., Danabasoglu, G., Donner, L. J., Holland, M. M., Hunke, E. C., Jayne, S. R., Lawrence, D. M., Neale, R. B., Rasch, P. J., and Vertenstein, M. (2011). The community climate system model version 4. Journal of Climate, 24 (19), 4973-4991.

Greve, P., Orlowsky, B., Mueller, B., Sheffield, J., Reichstein, M., & Seneviratne, S. I. (2014). Global assessment of trends in wetting and drying over land. Nature Geoscience, 7(10), 716-721.

Hansen, J., Ruedy, R., Sato, M., & Lo, K. (2010). Global surface temperature change. Reviews of Geophysics, 48(4).

Harris, I., Jones, P.D., Osborn, T.J. & Lister, D.H. (2014), Updated high-resolution grids of monthly climatic observations – the CRU TS3.10 Dataset. International Journal of Climatology, 34, 623–642.

Held, I. M., & Soden, B. J. (2006). Robust responses of the hydrological cycle to global warming. Journal of Climate, 19(21), 5686-5699.

Holmgren, M., Stapp, P., Dickman, C. R., Gracia, C., Graham, S., & Gutiérrez, J. R., et al. (2006). A synthesis of enso effects on drylands in australia, north america and south america. Advances in Geosciences, 6(6), 69-72.

Hu, Z., Chen, X., Chen, D., Li, J., Wang, S., Zhou, Q., Yin, G., and Guo, M. (2019), "Dry gets drier, wet gets wetter": A case study over the arid regions of central Asia, International Journal of Climatology, 39(2), 1072-1091.

Huang, J., Li, Y., Fu, C., Chen, F., Fu, Q., Dai, A., & Zhang, L. (2017). Dryland climate change: Recent progress and challenges. Reviews of Geophysics, 55(3), 719-778.

Huang, J., Yu, H., Guan, X., Wang, G., & Guo, R. (2016). Accelerated dryland expansion under climate change. Nature Climate Change, 6(2), 166.

Huang, X., Oberhansli, H., Von Suchodoletz, H., Prasad, S., Sorrel, P., Plessen, B., Mathis, M., & Usubaliev, R. (2014). Hydrological changes in western central asia (kyrgyzstan) during the holocene as inferred from a palaeolimnological study in lake son kul. Quaternary Science Reviews, 103, 134-152.

IPCC. (2013). Climate Change 2013: The Physical Science Basis. Contribution of Working Group I to the Fifth Assessment Report of the Intergovernmental Panel on Climate Change. Cambridge University Press, Cambridge, United Kingdom.

King, A. D., Donat, M. G., Alexander, L. V., & Karoly, D. J. (2014). The enso-australian rainfall teleconnection in reanalysis and cmip5. Climate Dynamics, 44(9-10), 2623-2635.

Kobayashi, S., Ota, Y., Harada, Y., Ebita, A., Moriya, M., Onoda, H., Onogi, K., Kamahori, H., Kobayashi, C., Endo, H., Miyaoka, K., & Takahashi, K. (2015). The JRA-55 Reanalysis: general specifications and basic characteristics. Journal of the Meteorological Society of Japan. 93, 5-48.

Kohfeld, K. E., Graham, R. M., Boer, A. M. D., Sime, L. C., Wolff, E. W., Quéré, C. L., & Boop, L. (2013). Southern hemisphere westerly wind changes during the last glacial maximum: paleo-data synthesis. Quaternary Science Reviews, 68(15), 76-95.

Lachniet, M. S., Denniston, R. F., Asmerom, Y., & Polyak, V. J. (2014). Orbital control of western north america atmospheric circulation and climate over two glacial cycles. Nature Communications, 5:3805.

Lehner, B., & Grill G. (2013). Global river hydrography and network routing: baseline data and new approaches to study the world's large river systems. Hydrological Processes, 27(15), 2171–2186.

Lézine, A. M., Hély, C., Grenier, C., Braconnot, P., & Krinner, G. (2011). Sahara and Sahel vulnerability to climate changes, lessons from Holocene hydrological data. Quaternary Science Reviews, 30(21-22), 3001-3012.

Li, Y., & Morrill, C. (2013). Lake levels in Asia at the Last Glacial Maximum as indicators of hydrologic sensitivity to greenhouse gas concentrations. Quaternary Science Reviews, 60, 1-12.

Li, Y., Liu, Y., Ye, W., Xu, L., Zhu, G., Zhang, X., & Zhang, C. (2018). A new assessment of modern climate change, China—An approach based on paleo-climate. Earth-Science Reviews, 177, 458-477.

Li, Y., Wang, Y. G., Houghton, R. A., & Tang, L. S. (2015). Hidden carbon sink beneath desert. Geophysical Research Letters, 42(14), 5880-5887.

Li, Y., Zhang, C., Wang, N., Han, Q., Zhang, X., Liu, Y., Xu, L., & Ye, W. (2017). Substantial inorganic carbon sink in closed drainage basins globally. Nature Geoscience, 10(7), 501-506.

Ljungqvist, F. C., Krusic, P. J., Sundqvist, H. S., Zorita, E., Brattstr, M, G., & Frank, D. (2016). Northern hemisphere hydroclimate variability over the past twelve centuries. Nature, 532(7597), 94-98.

Lorenz, D. J., Nieto-Lugilde, D., Blois, J. L., Fitzpatrick, M. C., & Williams, J. W. (2016). Downscaled and debiased climate simulations for North America from 21,000 years ago to 2100AD. Scientific data, 3, 160048.

Lowry, D. P., & Morrill, C. (2019). Is the Last Glacial Maximum a reverse analog for future hydroclimate changes in the Americas?. Climate Dynamics, 52(7-8), 4407-4427.

Magee, J. W., Miller, G. H., Spooner, N. A., & Questiaux, D. (2004). Continuous 150 ky monsoon record from Lake Eyre, Australia: insolation-forcing implications and unexpected Holocene failure. Geology, 32(10), 885-888.

Masutomi, Y., Inui, Y., Takahashi, K. & Matsuoka, Y. (2009). Development of highly accurate global polygonal drainage basin data. Hydrological Processes, 23, 572–584.

Quade, J., & Broecker, W. S. (2009). Dryland hydrology in a warmer world: Lessons from the Last Glacial period. The European Physical Journal Special Topics, 176(1), 21-36.

Ran, M., & Feng, Z. (2013). Holocene moisture variations across china and driving mechanisms: a synthesis of climatic records. Quaternary International, 313-314, 179-193.

Rana, S., Mcgregor, J., & Renwick, J. (2017). Wintertime precipitation climatology and enso sensitivity over central southwest asia. International Journal of Climatology, 37(3).

Roderick, M., Sun, F., Lim, W. H., & Farquhar, G. (2014). A general framework for understanding the response of the water cycle to global warming over land and ocean. Hydrology and Earth System Sciences, 18, 1575–1589.

Schmidt, G. A., Kelley, M., Nazarenko, L., Ruedy, R., Russell, G. L., Aleinov, I., Bauer, M., Bauer, S. E., Bhat, M. K., and Bleck, R. (2014). Configuration and assessment of the GISS ModelE2 contributions to the CMIP5 archive. Journal of Advances in Modeling Earth Systems, 6(1), 141-184.

Shakun, J. D., & Carlson, A. E. (2010). A global perspective on Last Glacial Maximum to Holocene climate change. Quaternary Science Reviews, 29(15-16), 1801-1816.

Street, F. A., & Grove, A. T. (1979). Global maps of lake-level fluctuations since 30,000 yr BP. Quaternary Research, 12(1), 83-118.

Street-Perrott, F.A., Marchand, D.S., Roberts, N., & Harisson, S.P. (1989). Global Lake-Level Variations from 18,000 to 0 Years Ago: A Paleoclimatic Analysis. U.S. Department of Energy Technical Report 46, Washington, D.C. 20545. Distributed by National Technical Information Service, Springfield, VA 22161.

Tabor, K., & Williams, J. W. (2010). Globally downscaled climate projections for assessing the conservation impacts of climate change. Ecological Applications, 20(2), 554-565.

Taylor, K. E., Stouffer, R. J., & Meehl, G. A. (2012). An overview of CMIP5 and the experiment design. Bulletin of the American Meteorological Society, 93(4), 485-498.

Tierney, J. E., Smerdon, J. E., Anchukaitis, K. J., & Seager, R. (2013). Multidecadal variability in east african hydroclimate controlled by the indian ocean. Nature, 493(7432), 389-392.

Trenberth, K. E., Dai, A., Schrier, G. V. D., Jones, P. D., Barichivich, J., Briffa, K. R., & Sheffield, J. (2013). Global warming and changes in drought. Nature Climate Change, 4(1), 17-22.

UNEP. (1992). World Atlas of Desertification. Edward Arnold, London.

Voldoire, A., Sanchez-Gomez, E., Salas y Mélia, D., Decharme, B., Cassou, C., Sénési, S., Valcke, S., Beau, I., Alias, A., Chevallier, M., Déqué, M., Deshayes, J., Douville, H., Fernandez, E., Madec, G., Maisonnave, E., Moine, M.-P., Planton, S., Saint-Martin, D., Szopa, S., Tyteca, S., Alkama, R., Belamari, S., Braun, A., Coquart, L., and Chauvin, F. (2013). The CNRM-CM5.1 global climate model: description and basic evaluation. Climate Dynamics, 40(9), 2091-2121.

Wang, G., Garcia, D., Liu, Y., De Jeu, R., & Dolman, A. J. (2012). A three-dimensional gap filling method for large geophysical datasets: Application to global satellite soil moisture observations. Environmental Modelling & Software, 30, 139-142.

Wang, J., Song, C., Reager, J. T., Yao, F., Famiglietti, J. S., Sheng, Y., MacDonald, G. M., Brun, F., Schmied, H. M., Marston, R. A., & Wada, Y. (2018). Recent global decline in endorheic basin water storages. Nature Geoscience, 11(12), 926-932.

Wang, P. X., Wang, B., Cheng, H., Fasullo, J., Guo, Z. T., Kiefer, T., & Liu, Z. Y. (2014). The global monsoon across timescales: coherent variability of regional monsoons. Climate of the Past, 10(6), 2007.

Watanabe, S., Hajima, T., Sudo, K., Nagashima, T., Takemura, T., Okajima, H., Nozawa, T., Kawase, H., Abe, M., and Yokohata, T. (2011). MIROC-ESM 2010: Model description and basic results of CMIP5-20c3m experiments. Geoscientific Model Development, 4(4), 845.

Wilby, R. L., Charles, S. P., Zorita, E., Timbal, B., Whetton, P., & Mearns, L. O. (2004). Guidelines for use of climate scenarios developed from statistical downscaling methods.

Wurtsbaugh, W. A., Miller, C., Null, S. E., DeRose, R. J., Wilcock, P., Hahnenberger, M., Howe, F., & Moore, J. (2017). Decline of the world's saline lakes. Nature Geoscience, 10(11), 816-821.

Xi, C., Wang, S., Hu, Z., Zhou, Q., & Qi, H. (2018). Spatiotemporal characteristics of seasonal precipitation and their relationships with enso in central asia during 1901–2013. Journal of Geographical Sciences, 28(9), 1341-1368.

Xue, B., Yu, G., & Zhang, F. J.(2017). Late quaternary lake database in China. Science Press, Beijing, China.

Yu, G., Harrison, S. P., & Xue, B. (2001). Lake status records from China: data base documentation. MPI-BGC Tech Rep 4.

Yukimoto, S., Adachi, Y., Hosaka, M., Sakami, T., Yoshimura, H., Hirabara, M., Tanaka, T. Y., Shindo, E., Tsujino, H., and Deushi, M. (2012). A new global climate model of the Meteorological Research Institute: MRI-CGCM3: Model description and basic performance. Journal of the Meteorological Society of Japan, 90, 23-64.

Zhan, S., Song, C., Wang, J., Sheng, Y., & Quan, J. (2019). A global assessment of terrestrial evapotranspiration increase due to surface water area change. Earth's future, 7(3), 266-282.

Zhang E, Zhao C, Xue B, Liu, Z., Yu, Z., Chen, R., & Shen, J.. (2017). Millennial-scale hydroclimate variations in southwest China linked to tropical Indian Ocean since the Last Glacial Maximum. Geology, 45(5), 435-438.